

# State-Insensitive Trapping of Single Atoms in Cavity QED

J. McKeever, J. R. Buck, A. D. Boozer, A. Kuzmich, H.-C. Nägerl, D. M. Stamper-Kurn, and H. J. Kimble  
*Norman Bridge Laboratory of Physics 12-33  
 California Institute of Technology, Pasadena, CA 91125*

Single Cesium atoms are cooled and trapped inside a small optical cavity by way of a novel far-off-resonance dipole-force trap (FORT), with observed lifetimes of 2 – 3 seconds. The trapping field is provided by a TEM<sub>00</sub> mode of the cavity at a wavelength of 935.6 nm, and is such that the external potential for the center-of-mass motion is only weakly dependent on the atom’s internal state. Continuous real time observations of single trapped atoms in a regime of strong coupling are reported, with mean duration 0.4 s and with individual events lasting  $\simeq 1$  s.

A long-standing ambition in the field of cavity quantum electrodynamics (QED) has been to trap single atoms inside high- $Q$  cavities in a regime of strong coupling [1]. Diverse avenues have been pursued for creating the trapping potential for atom confinement, including the use of additional far off-resonant trapping beams [2], of the cavity QED light itself [3, 4], and of single trapped ions in high-finesse optical cavities [5, 6]. A critical aspect of this research is the development of techniques for atom localization that are compatible with strong coupling and that do not interfere with cavity QED interactions, as is required for schemes proposed for quantum computation and communication via cavity QED [7, 8, 9, 10, 11, 12].

The experiments described in this Letter constitute important steps forward in enabling quantum information processing in cavity QED by (1) achieving extended trapping times for single atoms in cavity QED in a regime of strong coupling, (2) realizing a trapping potential for the center-of-mass motion that is largely independent of the internal atomic state, and (3) demonstrating a scheme that allows continuous observation of a strongly coupled trapped atom. More specifically, we have recorded trapping times up to 3 s for single Cs atoms stored in an intracavity far-off resonance trap (FORT) [13], which represents an improvement by a factor of  $10^2$  beyond the first realization of trapping in cavity QED [2], and by roughly  $10^4$  beyond prior results for atomic trapping [3] and localization [4] by way of the cavity QED field itself. Although our longest lifetimes are obtained when near-resonant fields are turned off, atoms can also be continuously monitored, leading to mean trapping times of 0.4 s, with some atoms observed for over 1 s. These observations as well as cooling and trapping protocols are facilitated by the choice of a “magic” wavelength for the FORT [14, 15, 16]. Unlike typical FORTs, where the signs of the AC-Stark shifts for excited and ground states are opposite, our trap causes small shifts to the relevant transition frequencies, thereby providing advantages for coherent state manipulation of the atom-cavity system.

Principal parameters relevant to cavity QED are the Rabi frequency  $2g_0$  for a single quantum of excitation and the amplitude decay rates  $(\kappa, \gamma)$  due to cavity losses and atomic spontaneous emission. For our system,  $g_0/(2\pi) = 24$  MHz and  $(\kappa, \gamma)/(2\pi) = (4.2, 2.6)$  MHz, where  $g_0$  is for the  $(6S_{1/2}, F = 4, m_F = 4) \rightarrow (6P_{3/2}, F' =$

$5, m'_F = 4)$  transition in atomic Cs at  $\lambda_0 = 852.4$  nm. Strong coupling is thereby achieved ( $g_0 \gg (\kappa, \gamma)$ ), as expressed by the critical photon and atom numbers ( $n_0 \equiv \gamma^2/(2g_0^2)$ ,  $N_0 \equiv 2\kappa\gamma/g_0^2$ )  $\simeq (0.006, 0.04) \ll 1$ .

Our experimental setup is schematically depicted in Fig. 1 [2]. The input to the cavity consists of cavity-QED probe, FORT-trapping, and cavity-locking beams, all of which are directed to separate detectors at the output. The transmitted probe beam is monitored using heterodyne detection, allowing real-time detection of individual cold atoms within the cavity mode [17]. The cavity length is actively controlled using a cavity resonance at  $\lambda_C = 835.8$  nm, so the length is stabilized and tunable independently of all other intracavity fields [2]. The cavity-QED probe fields as well as the FORT beam are linearly polarized along a direction  $\hat{l}_+$  orthogonal to the  $x$ -axis of the cavity [18, 19].

Cold atoms are collected in a magneto-optical trap (MOT) roughly 5 mm above the cavity mirrors and then released after a stage of sub-Doppler polarization-gradient cooling [13]. Freely falling atoms arrive at the cavity mode over an interval of about 10 ms, with kinetic energy  $E_K/k_B \simeq 0.8$  mK, velocity  $v \simeq 0.30$  m/s, and transit time  $\delta t = 2w_0/v \simeq 150$   $\mu$ s. Two additional orthogonal pairs of counter-propagating beams in a  $\sigma^+ - \sigma^-$  configuration illuminate the region between the cavity mirrors along directions at  $\pm 45^\circ$  relative to

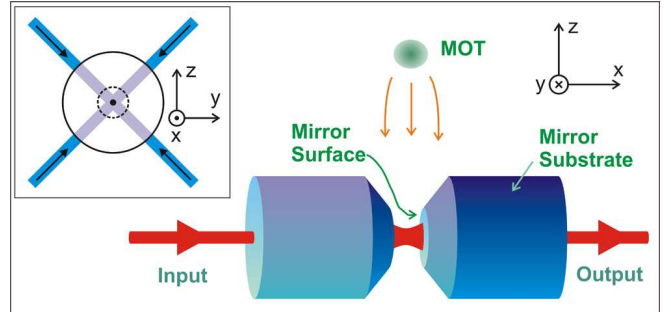


FIG. 1: Schematic of experiment for trapping single atoms in cavity QED. Relevant cavity parameters are length  $l = 43.0$   $\mu$ m, waist  $w_0 = 23.9$   $\mu$ m, and finesse  $\mathcal{F} = 4.2 \times 10^5$  at 852 nm. The inset illustrates transverse beams used for cooling and repumping.

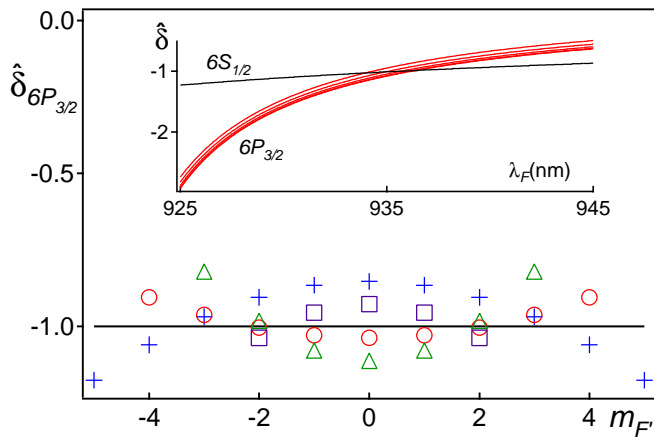


FIG. 2: AC-Stark shifts ( $\hat{\delta}_{6S_{1/2}}, \hat{\delta}_{6P_{3/2}}$ ) for the ( $6S_{1/2}, 6P_{3/2}$ ) levels in atomic Cs for a linearly polarized FORT. The inset shows ( $\hat{\delta}_{6S_{1/2}}, \hat{\delta}_{6P_{3/2}, F'=4}$ ) as functions of FORT wavelength  $\lambda_F$ . The full plot gives  $\hat{\delta}_{6P_{3/2}}$  versus  $m_{F'}$  for each of the levels  $6P_{3/2}, F' = 2, 3, 4, 5$  for  $\lambda_F = 935.6$  nm. In each case, the normalization is  $\hat{\delta} = \delta / [\delta_{6S_{1/2}}(\lambda_F = 935.6 \text{ nm})]$  [21].

$\hat{y}, \hat{z}$  (the “ $y-z$  beams”) and contain cooling light tuned red of  $F = 4 \rightarrow F' = 5$  and repumping light near the  $F = 3 \rightarrow F' = 3$  transition [20]. These beams eliminate the free-fall velocity to capture atoms in the FORT and provide for subsequent cooling of trapped atoms.

A major obstacle to the integration of a conventional red-detuned FORT with cavity QED is that excited electronic states generally experience a positive AC-Stark shift of comparable magnitude to the negative (trapping) shift of the ground state [13]. This leads to the unfortunate consequence that the effective detuning between an atomic transition and the cavity mode becomes a strong function of the atom’s position within the trap, which interferes with the cavity QED interactions [16]. However, due to the specific multi-level structure of Cs, the wavelength  $\lambda_F$  of the trapping laser can be tuned to a region where both of these problems are eliminated [14, 15], as illustrated in Fig. 2 [21]. Around the “magic” wavelength  $\lambda_F = 935$  nm, the sum of AC-Stark shifts coming from different allowed optical transitions results in the ground  $6S_{1/2}$  and excited  $6P_{3/2}$  states both being shifted downwards by comparable amounts,  $\delta_{6S_{1/2}} \simeq \delta_{6P_{3/2}}$ . The AC-Stark shifts remain slightly dependent on the hyperfine and magnetic quantum numbers of the  $6P_{3/2}$  states, as shown in Fig. 2.

Our cavity has a TEM<sub>00</sub> longitudinal mode located nine orders below the cavity QED mode, at the wavelength  $\bar{\lambda}_F = 935.6$  nm, allowing the implementation of an internal-state insensitive FORT. The field to excite this cavity mode is provided by a laser at  $\bar{\lambda}_F$ , which is independently locked to the cavity. The finesse of the cavity at  $\bar{\lambda}_F$  is  $\mathcal{F} \sim 2200$  [19], so that a mode-matched input power of 1.2 mW gives a peak AC-Stark shift  $\delta_{6S_{1/2}} = -47$  MHz for all states in the  $6S_{1/2}$  ground manifold, corresponding to a trap depth  $U_0/k_B = 2.3$  mK,

which was used for all of our experiments.

We employed two distinct protocols to study the lifetime for trapped atoms in our FORT. In the first, we use the  $F = 4 \rightarrow F' = 5$  transition for cavity QED interactions with zero detuning of the cavity from the bare atomic resonance,  $\Delta_C \equiv \omega_C - \omega_{4 \rightarrow 5} = 0$ . In contrast to Ref. [2], here the FORT is *ON* continuously without switching, which makes a cooling mechanism necessary to load atoms into the trap. The initial detection of a single atom falling into the cavity mode is performed with a probe beam tuned to the lower sideband of the vacuum-Rabi spectrum ( $\Delta_p = \omega_p - \omega_{4 \rightarrow 5} = -20$  MHz), generating an *increase* in transmitted probe power when an atom approaches a region of optimal coupling [22, 23]. This increase triggers *ON* a pulse of transverse cooling light from the  $y-z$  beams, detuned 41 MHz red of  $\omega_{4 \rightarrow 5}$ . During the subsequent trapping interval, all near-resonant fields are turned *OFF* (including the transverse cooling light), both via acousto-optical switches and mechanical shutters. After a variable delay  $t_T$ , the cavity-QED probe field is switched back *ON* to detect whether the atom is still trapped, where now  $\Delta_p = 0$ , resulting in a sharp *decrease* in transmission when an atom is present. These observations of single intracavity atoms in the FORT are enabled by the state-insensitive character of the trap.

Data collected in this manner are shown in Fig. 3(a), which displays the conditional probability  $P$  to detect an atom given an initial single-atom triggering event versus the time delay  $t_T$ . The two data sets shown in Fig. 3(a) yield comparable lifetimes, the upper having been acquired with mean intracavity atom number  $\bar{N} = 0.30$  atoms and the lower with  $\bar{N} = 0.019$  [24]. The offset in  $P$  between these two curves arises primarily from the reduction in  $\delta t$  of the cooling pulses, from 100  $\mu\text{s}$  to 5  $\mu\text{s}$ , which results in a reduced capture probability. In addition to determining the lifetime, such measurements with various loading conditions allow us to investigate the probability of trapping an atom other than the “trigger” atom and of capturing more than one atom. For example, with  $\delta t = 5 \mu\text{s}$  as in the lower set, we have varied  $0.011 \lesssim \bar{N} \lesssim 0.20$  with no observable change in either  $P_T$  or the trap lifetime  $\tau$ . Since a conservative upper bound on the relative probability of trapping a second atom is just  $\bar{N}$  itself (when  $\bar{N} \ll 1$ ), these data strongly support the conclusion that our measurements are for single trapped atoms. Quite generally, we routinely observe lifetimes in the range  $2 \text{ s} < \tau < 3 \text{ s}$  depending upon the parameters chosen for trap loading and cooling.

Fig. 3(b) explores scattering processes within the FORT that transfer population between the  $6S_{1/2}, F = (3, 4)$  ground-state hyperfine levels. For these measurements, the  $F = 4$  level is initially depleted, and then the population in  $F = 4$  as well as the total  $3+4$  population are monitored as functions of time  $t_D$  to yield the fractional population  $f_4(t_D)$  in  $F = 4$ . The measured time  $\tau_R = (0.11 \pm 0.02)\text{s}$  for re-equilibration of populations between  $F = (3, 4)$  agrees with a numerical simulation based upon the relevant scattering rates in our FORT,

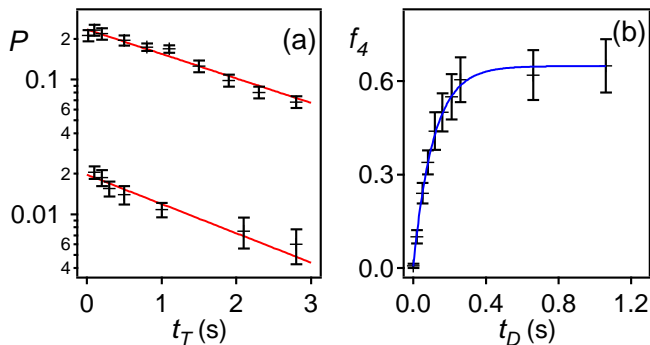


FIG. 3: (a) Detection probability  $P$  as a function of trapping time  $t_T$ . The upper data set is for mean intracavity atom number  $\bar{N} \approx 0.30$ , while the lower set is for  $\bar{N} \approx 0.019$  atoms. Exponential fits (solid lines) yield lifetimes  $\tau_{\text{upper}} = (2.4 \pm 0.2)$  s and  $\tau_{\text{lower}} = (2.0 \pm 0.3)$  s. (b) The fractional population  $f_4(t_D)$  in  $F = 4$  following depletion of this level at  $t = 0$ . An exponential fit (solid line) gives  $\tau_R = (0.11 \pm 0.02)$  s.

which predicts  $\tau_R = 0.10$  s for atoms trapped exactly at the peak FORT intensity and for an unpolarized initial state in the  $F = 4$  manifold.

Turning next to the question of the mechanisms that limit our FORT lifetime, we recall that in the work of Ref. [2], the lifetime  $\tau = 28$  ms was attributed to parametric heating caused by intensity fluctuations of the trapping field [25]. Since then, we have invested considerable effort to understand and eliminate this heating mechanism [26], which is characterized by an exponential temperature growth at rate  $\Gamma_p \equiv 1/\tau_p = \pi^2 \nu_{tr}^2 S_e(2\nu_{tr})$ , with  $S_e(2\nu_{tr})$  as the power spectral density of fractional intensity fluctuations evaluated at twice the (harmonic) trap frequency  $\nu_{tr}$ . In our FORT, the relevant harmonic frequencies are  $\nu_a = 570$  kHz for motion along the  $x$ -axis of the cavity and  $\nu_r = 4.8$  kHz in the radial  $y - z$  plane. However, due to the anharmonic shape of the FORT potential, as a trapped atom heats, its motion will include a wide spectrum of frequencies below  $(\nu_a, \nu_r)$ . We therefore estimate a lower bound to the FORT lifetime due to this heating mechanism by taking the maximum value of  $\Gamma_p$  over the frequency range of interest, leading to  $\tau_p^{\text{axial}} > 1.6$  s [27]. This estimate suggests that parametric heating could be a limiting factor in the lifetime recorded in Fig. 3. However, subsequent measurements of the FORT lifetime were performed in which the intensity noise was reduced below the shot-noise level of our detection system, giving a lower bound  $\tau_p^{\text{axial}} > 9$  s. Unfortunately, the measured lifetime was  $\tau = (3.1 \pm 0.4)$  s, indicating that other mechanisms are at least partially responsible for the observed decay rates.

A second suspect is a heating process described by Corwin *et al.* [28] associated with inelastic Raman scattering driven by the FORT field. For a linearly polarized FORT sufficiently far-detuned with respect to the ground-state hyperfine splitting, Zeeman sublevels in the  $6S_{1/2}, F = (3, 4)$  manifold are degenerate. However, this

degeneracy is lifted for any degree of elliptical polarization, which is present in our cavity due to residual mirror birefringence [18, 19]. State-changing Raman transitions driven by the FORT field can then lead to heating, since the sublevels are trapped in wells of different depths. We calculate rates  $\Gamma_s$  for spontaneous Raman scattering in our FORT to be 2.5 to 7  $\text{s}^{-1}$  for transitions that change the hyperfine quantum number  $F$ , and between 0.8 and 2.5  $\text{s}^{-1}$  when only  $m_F$  changes [29]. Based on Eq. 3 in Ref. [28] (a two-ground-state model), we can estimate an upper limit to the heating rate from this mechanism,  $\Gamma_R \lesssim 0.2\Gamma_s$ , giving heating timescales as short as 0.7 s for the fastest calculated scattering rate. These estimates indicate that this effect could indeed be important. However, we have also undertaken a more detailed calculation, including a full multilevel simulation of the optical pumping processes, which indicates a much slower heating rate,  $\Gamma_R \sim 0.02 \text{ s}^{-1}$ . We are working to resolve the difference between these calculations.

A third suspect that cannot be discounted is the presence of stray light, which we have endeavored to eliminate. For lifetimes as in Fig. 3, we require  $\bar{n} \ll 10^{-5}$ , which is not trivial to diagnose. A final concern is the background pressure in the region of the FORT. Although the pressure in the chamber is typically  $3 \times 10^{-10}$  Torr (leading to  $\tau \simeq 30$  s), we have no direct measurement of the residual gas density in the narrow cylinder between the mirror substrates (diameter 1 mm and length 43  $\mu\text{m}$ ), except for the trap lifetime itself.

The results presented above were obtained “in the dark” with the atom illuminated only by the FORT laser at  $\lambda_F$  and the cavity-locking laser at  $\lambda_C$ . Toward the goals of continuous observation of single trapped atoms over long times and of implementing  $\Lambda$ -schemes in cavity QED [7, 8, 9, 30], we next present results from a second protocol. In this scheme, the cavity is on resonance with the  $F = 4 \rightarrow F' = 4$  transition ( $\Delta'_C \equiv \omega_C - \omega_{4 \rightarrow 4} = 0$ ). Atoms falling into the cavity mode are detected by a reduction in probe transmission through the cavity ( $\Delta'_p = \omega_p - \omega_{4 \rightarrow 4} = 0$ ), with the probe then triggered *OFF*. Here, the repumping light from the transverse  $y - z$  beams is always *ON*, with fixed detuning  $\Delta_3$  with respect to the  $F = 3 \rightarrow F' = 3$  resonance. Cooling light from the  $y - z$  beams to drive  $F = 4 \rightarrow F' = 5$  is no longer used. After a delay of 80 ms following a trigger event (which allows other atoms to fall through the cavity and be lost), the probe beam is switched back *ON*, and sets  $t = 0$ . As before, the FORT is left *ON* continuously.

An example of the resulting probe transmission is shown in Fig. 4, which displays the continuous observation of a single trapped atom. In these experiments, unlike those of Fig. 3, we use lower detection bandwidth (1 kHz instead of 30 kHz) since the probe power is much weaker ( $\bar{m}_e \simeq 0.02$  instead of  $\simeq 0.5$  for the empty cavity). This reduced time resolution for the trigger in the presence of continuous probing and repumping fields means that we trap more than one atom with increased frequency, as evidenced by probe transmission below the

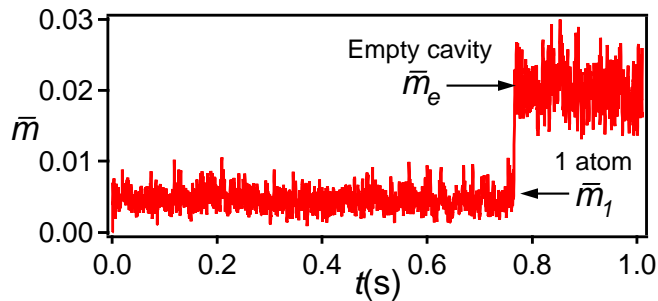


FIG. 4: Continuous observation of a single atom trapped inside a cavity in a regime of strong coupling. Displayed is the strength of the intracavity field  $\bar{m} = |\langle \hat{a} \rangle|^2$  deduced from the heterodyne current as a function of time  $t$ , where the initial trigger event occurred at  $t = -80$  ms. RF detection bandwidth = 1 kHz,  $\Delta'_C = 0 = \Delta'_p$ , and  $\Delta_3 = 25$  MHz (*blue*).

level  $\bar{m}_1$  of Fig. 4. In such cases, the probe transmission versus  $t$  is observed always to increase in a discontinuous “staircase” of steps, presumably due to the loss of successive atoms, with the last level before  $\bar{m}_e$  corresponding to  $\bar{m}_1$ , which we then associate with a single atom.

Given that the FORT is *ON* continuously, it is remarkable that a falling atom can be trapped and observed over long intervals as in Fig. 4 in the *absence* of transverse cooling light on the  $F = 4 \rightarrow F' = 5$  transition. Since we have not seen such striking phenomena under similar conditions for cavity QED with the  $F = 4 \rightarrow F' = 5$  transition, it seems likely that a cycle between hyperfine ground levels  $F = 3 \leftrightarrow 4$  is involved in a cooling process involving the repumping and cavity-QED beams. We observe a strong dependence of the trapping and continuous observation times on the detuning of the  $y - z$  repump-

ing beams near  $F = 3 \rightarrow F' = 3$ , with an optimal value  $\Delta_3 \simeq 25$  MHz to the *blue*, which strongly suggests blue Sisyphus cooling as has been employed in “gray” optical molasses [31]. The cavity QED probe is also a critical component, since without it, observations as in Fig. 4 are not possible, although it is not clear whether this beam is acting as a simple “repumper” or is functioning in a more complex fashion due to strong coupling.

In summary, we have demonstrated trapping of single atoms in a domain of strong coupling in cavity QED. Lifetimes of  $\tau \simeq 2 - 3$  seconds have been achieved, and are limited by as yet unidentified loss mechanisms. Since intrinsic heating in the FORT is quite low ( $\sim 11$   $\mu\text{K/s}$  due to photon recoil), we anticipate possible extensions to much longer lifetimes. The small transition shifts for our FORT should enable the application of a variety of laser cooling schemes, including for atomic confinement in the Lamb-Dicke regime. The realization of this FORT also sets the stage for further advances in quantum information science via photon-atom interactions. For example, for an atom trapped in our FORT, the rate of optical information  $\mathcal{R} \equiv g_0^2/\kappa \sim 10^9/\text{s} \gg (\kappa, \gamma)$ , leading to information about atomic dynamics at a rate that far exceeds that from either cavity decay at rate  $\kappa$  or spontaneous scattering at rate  $\gamma$  (as in fluorescence imaging) and suggesting new possibilities for sensing and control of the quantum dynamics of an individual system.

We gratefully acknowledge the contributions of K. Birnbaum, A. Boca, T. W. Lynn, S. J. van Enk, D. W. Vernooy, and J. Ye. This work was supported by the Caltech MURI Center for Quantum Networks under ARO Grant No. DAAD19-00-1-0374, by the National Science Foundation, and by the Office of Naval Research.

- 
- [1] For a review, see contributions in the special issue of Phys. Scr. T76, 127 (1998).
- [2] J. Ye *et al.*, Phys. Rev. Lett. **83**, 4987 (1999); and D. W. Vernooy, Doctoral Thesis (California Institute of Technology, 2000).
- [3] C. J. Hood *et al.*, Science **287**, 1447 (2000); Phys. Rev. A **63**, 013401 (2000).
- [4] P. W. H. Pinkse *et al.*, Nature **404**, 365 (2000).
- [5] G. R. Guthöhrlein *et al.*, Nature **414**, 49 (2001).
- [6] J. Eschner *et al.*, Nature **413**, 495 (2001).
- [7] T. Pellizari *et al.*, Phys. Rev. Lett. **75**, 3788 (1995).
- [8] J. I. Cirac *et al.*, Phys. Rev. Lett. **78**, 3221 (1997).
- [9] S. van Enk *et al.*, Fortschr. Phys. **46**, 689 (1998).
- [10] C. Cabrillo *et al.*, Phys. Rev. A **59**, 1025 (1999).
- [11] S. Bose *et al.*, Phys. Rev. Lett. **83**, 5158 (1999).
- [12] A. S. Parkins and H. J. Kimble, Journal Opt. B: Quantum Semiclass. Opt. **1**, 496 (1999).
- [13] *Laser Cooling and Trapping*, H. J. Metcalf and P. van der Straten (Springer-Verlag, 1999).
- [14] C. J. Hood and C. Wood as described in H. J. Kimble *et al.*, *Laser Spectroscopy XIV*, eds. Rainer Blatt *et al.* (World Scientific, Singapore, 1999), 80.
- [15] H. Katori *et al.*, J. Phys. Soc. Jpn. **68**, 2479 (1999); T. Ido *et al.*, Phys. Rev. A **61**, 061403 (2000).
- [16] S.J. van Enk *et al.*, Phys. Rev. A **64**, 013407 (2001).
- [17] H. Mabuchi *et al.*, Opt. Lett. **21**, 1393 (1996).
- [18] Because of small stress-induced birefringence in the cavity mirrors, we attempt to align the directions of linear polarization for the FORT and cavity QED fields along an axis that coincides with one of the cavity eigenpolarizations [19], denoted by  $\hat{l}_{\pm}$ . For initial polarization along  $\hat{l}_+$ , measurements of FORT [cavity-QED probe] polarization along  $\hat{l}_-$  for the cavity output power  $P$  give  $P_-/P_+ < 0.02[0.002]$  for the FORT [cavity-QED] beam.
- [19] C. J. Hood *et al.*, Phys. Rev. A **64**, 033804 (2001).
- [20] We estimate the (incoherent) sum of the four intensities to be  $I_{4-5} \sim 60\text{mW/cm}^2$  for the cooling and  $I_{3-3} \sim 40\text{mW/cm}^2$  for the repumping light, with uncertainties of roughly a factor of 2.
- [21] To compute the shifts shown in Fig. 2, we have used an extended model that includes counter-rotating terms and the following couplings:  $6S_{1/2} \rightarrow nP_{1/2,3/2}$ , for  $n = 6 - 11$ ;  $6P_{3/2} \rightarrow nS_{1/2}$  for  $n = 6 - 15$ ;  $6P_{3/2} \rightarrow nD_{3/2,5/2}$  for  $n = 5 - 11$ . Relevant parameters are taken principally

- from C. J. Hood, Doctoral Thesis (California Institute of Technology, 2000) and references therein and from M. Fabry and J. R. Cussenot, *Can. J. Phys.* **54**, 836 (1976).
- [22] C. J. Hood *et al.*, *Phys. Rev. Lett.* **80**, 4157 (1998).
- [23] Specific examples of single-atom detection events are omitted here. The up-going increases in cavity transmission are quite similar to those in Refs. [3, 22], while the down-going events are similar to those in Refs. [2, 17], albeit now in the presence of the FORT.
- [24] Estimates of  $\bar{N}$  are obtained from the mean number of atom transit events (each of duration  $\simeq 150\mu\text{s}$ ) during the interval  $\simeq 10\text{ms}$  from the falling MOT atoms, in the absence of trapping.
- [25] T. A. Savard *et al.*, *Phys. Rev. A* **56**, R1095 (1997); C. W. Gardiner *et al.*, *ibid.* **61**, 045801 (2000).
- [26] J. McKeever and H. J. Kimble, in *Laser Spectroscopy XIV*, eds. S. Chu and J. Kerman (World Scientific, 2002).
- [27] The predicted  $\tau_p^{radial} > 10^4$  s, suggesting that parametric heating in the radial direction is not an issue.
- [28] K. L. Corwin *et al.*, *Phys. Rev. Lett.* **83**, 1311 (1999).
- [29] R. A. Cline *et al.*, *Opt. Lett.* **19**, 207 (1994).
- [30] A. Kuhn *et al.*, *Phys. Rev. Lett.* **89**, 067901 (2002).
- [31] D. Boiron *et al.*, *Phys. Rev. A* **53**, R3734 (1996) and references therein.